Brain Stimulation 12 (2019) 1169–1176

Contents lists available at ScienceDirect

Brain Stimulation

journal homepage: http://www.journals.elsevier.com/brain-stimulation

Cerebellar transcranial direct current stimulation modulates the fMRI signal in the cerebellar nuclei in a simple motor task

Michael Küper [a, *], Jahan Saeed Mallick [a], Thomas Ernst [a], Oliver Kraff [b, c], Markus Thürling [a], Maria Roxana Stefanescu [a], Sophia Göricke [b], Michael A. Nitsche [d, e], Dagmar Timmann [a]

[a] Department of Neurology, University of Duisburg-Essen, Hufelandstrasse 55, 45122, Essen, Germany
[b] Institute of Diagnostic and Interventional Radiology and Neuroradiology, University of Duisburg-Essen, Hufelandstrasse 55, 45122, Essen, Germany
[c] Erwin L. Hahn Institute for Magnetic Resonance Imaging, Kokereiallee 7, Building C84 UNESCO World Heritage, Zeche Zollverein, 45141, Essen, Germany
[d] Department of Psychology and Neurosciences, Leibniz Research Centre for Working Environment and Human Factors, Ardeystr.67, 44139, Dortmund, Germany
[e] Department of Neurology, University Medical Hospital Bergmannsheil, Bürkle de la Camp-Platz 1, 44789, Bochum, Germany

ARTICLE INFO

Article history:
Received 12 August 2016
Received in revised form
31 March 2019
Accepted 1 April 2019
Available online 4 April 2019

Keywords:
Cerebellum
tDCS
fMRI
Finger tapping
Dentate nucleus

ABSTRACT

Background: In a seminal paper, Galea et al. (Modulation of cerebellar excitability by polarity-specific noninvasive direct current stimulation. 2009. J Neurosci *29*, 9115–9122) showed that cerebellar transcranial direct current stimulation (ctDCS) alters cerebellar-M1 connectivity. This effect has been explained by ctDCS-related changes of excitability of the cerebellar cortex with consecutive modulation of its main output, the dentate-thalamo-cortical pathway.
Objectives: The aim of this functional magnetic resonance imaging (fMRI) study was to provide evidence that cathodal ctDCS decreases the activity of the cerebellar cortex, resulting in increased activity of the cerebellar nuclei, whereas anodal ctDCS has the opposite effect.
Methods: A total of 48 participants (female/male: 23/25, age: 23.8 ± 4.1yrs., mean ± standard deviation) performed a finger tapping task with the right hand in a 3T MRI scanner. Functional MR images were acquired prior, during and after tDCS of the right cerebellum. Participants were assigned randomly to anodal, cathodal or sham ctDCS.
Results: No significant difference of cerebellar cortical activation was found after comparing the three modes of stimulation. On the level of the dentate nuclei, however, a significant increase of activation was detected during and after cathodal stimulation. Furthermore, dentate nuclei activation was suppressed on a trend level following anodal stimulation.
Conclusions: The present findings support the hypothesis that cathodal ctDCS leads to a disinhibition of the dentate nucleus, whereas anodal ctDCS may have the opposite effect.

Introduction

Cerebellar transcranial direct current stimulation (ctDCS) is a non-invasive brain stimulation technique that has been shown to modulate motor and non-motor functions in healthy subjects [see for 1 review]. It has been found to affect motor-adaptation [2–5], working-memory performance [6,7], procedural learning [8], eye-blink conditioning [9], and other cognitive and motor processes [10]. Furthermore, a reduction of the severity of ataxia symptoms has been reported in cerebellar patients following ctDCS [11–13].

The various effects of ctDCS are thought to depend on stimulation-induced neuronal excitability changes. Nitsche and Paulus [14] demonstrated an excitatory effect of anodal stimulation over the motor cortex (M1) and an inhibitory effect of cathodal stimulation. These effects are present during stimulation (so called direct effects, online stimulation) and for up to 90 min after stimulation (after effects, offline stimulation) [15].

Because the cerebellar cortex is highly convoluted and the neuronal architecture is different, cerebellar tDCS effects are not necessarily the same as M1 tDCS effects. In order to assess

* Corresponding author.
E-mail address: Michael.Kueper@uni-due.de (M. Küper).

https://doi.org/10.1016/j.brs.2019.04.002
1935-861X/

cerebellar cortical excitability changes, Galea et al. [16] studied the effect of ctDCS on cerebello-brain-inhibition (CBI). The concept of CBI postulates an inhibitory tone of the cerebellar cortex over M1 mediated via the cerebellar nuclei and the thalamus. While the cerebellar cortical Purkinje cells have an inhibitory GABAergic effect on the cerebellar nuclei, there is a disynaptic excitatory output from the cerebellar nuclei to M1 relayed via the thalamus [17]. The concept of CBI is based on studies showing that a conditioning transcranial magnetic stimulation (TMS) pulse applied over the cerebellum prior to TMS of M1 reduces motor evoked potential (MEP) amplitudes, due to TMS-induced activation of Purkinje cells, which inhibit the excitatory drive of cerebellar nuclei to the primary motor cortex [1,18]. In accordance, excitatory anodal ctDCS increased the ability of TMS to elicit CBI, whereas cathodal ctDCS decreased it [16]. It was suggested that this effect is caused by increased excitability of cerebellar cortical Purkinje cells due to anodal ctDCS, whereas cathodal ctDCS has an opposite effect. The aim of the present study was to further confirm this assumption using functional magnetic resonance imaging (fMRI). Previous studies have shown that fMRI signals are modulated by tDCS. For example, Stagg et al. [19] reported a significant increase of M1 activation after anodal tDCS. Changes of cerebellar activation have also been reported during a working memory task following anodal ctDCS [20].

We investigated changes of activity of the cerebellar cortex and the dentate nuclei in response to tDCS over the cerebellar cortex during a simple motor task using fMRI. Direct and after effects of tDCS were explored. We hypothesized that cathodal ctDCS would lead to a decrease of cerebellar cortical activity which would result in decreased inhibition of the dentate nucleus. As a consequence, the fMRI signal of the dentate nucleus should increase. Opposite effects were expected for anodal stimulation.

Materials and methods

Participants

54 healthy participants were included in the study. Exclusion criteria were neurological (including epilepsy) or psychiatric disorders, contraindications for MRI scanning and ages under 18 years. Informed consent was obtained from all participants. All participants were right-handed as assessed by the Edinburgh handedness scale [21]. The study was approved by the local ethics committee. Two participants were excluded because they did not complete the study (one participant reported discomfort during MRI acquisition; one MRI session had to be stopped due to technical problems). Three participants were excluded because of MRI-artifacts (Nyquist N/2 ghosts). One participant was excluded because of an incidental finding of a pons glioma.

fMRI scanning

A whole-body 3 T MRI scanner (Magnetom Biograph mMR, Siemens Healthcare, Erlangen, Germany) was used to acquire blood-oxygenation-level-dependent (BOLD)-contrast-weighted echo-planar images (EPIs) for functional scans. Head movements were reduced with the help of wedge-shaped bolsters. All fMRI images were acquired with an 8-channel head-neck coil (Siemens Healthcare, Erlangen, Germany). The scans covered the entire cerebellum. Each EPI session consisted of 200 scans (TR = 3000 ms, TE = 35 ms, Voxel size $2.2 \times 2.2 \times 2.0\ mm^3$). Because of magnetization relaxation effects, the first 5 vol in each session were discarded from further analysis. In addition, a three-dimensional (3D) transverse volume of the entire brain was acquired using a T1-weighted magnetization prepared rapid acquisition gradient echo sequence (MPRAGE, TR 2500 ms, TE 4.37 ms, voxel size $1 \times 1 \times 1\ mm^3$). Correct tDCS electrode position over the right cerebellar hemisphere was controlled in the MR scout image before fMRI sessions started (Fig. 1).

Participants performed a simple motor task (finger tapping) with the right hand. The participants' arm rested on the right thigh. Finger tapping was performed with the right index finger with repeated lateral movements consisting of two taps to the right side followed by one tap to the left side. Participants could perform the task at their own pace, yet a frequency of 2–3 Hz was suggested. Task performance was trained with participants inside the scanner prior to imaging. Correct task performance was controlled by visual inspection from the MRI control room. A block design was used consisting of eleven 30 s rest periods and nine 30 s periods of activity. Task performance and rest conditions were conducted with open eyes. An active block was started by visual presentation of the word “finger” in the centre of the participants' visual field. During rest, a fixation cross was presented in the same location. Visual stimuli were generated by a PC system running “Presentation” software (www.neurobs.com) and presented via a projector onto a

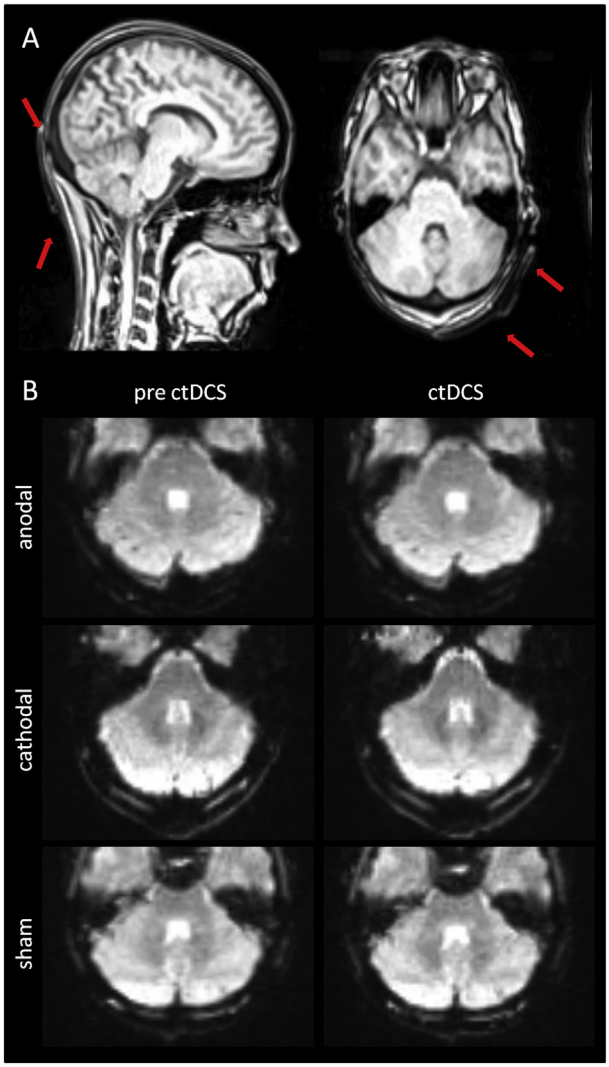

Fig. 1. A) MRI-Scout performed at the beginning of the MRI-session and used to control for correct electrode placement (red arrows) over the right cerebellar hemisphere. B) Typical examples of cerebellar EPI images during anodal, cathodal and sham ctDCS. . (For interpretation of the references to colour in this figure legend, the reader is referred to the Web version of this article.)

screen. Images were viewed from a mirror mounted on the eight-channel head-neck coil. Three cycles (pre-stimulation, stimulation, post-stimulation) of fMRI scanning were performed. During the same MRI session, resting state fMRI was acquired as part of another study. Table 1 shows the order of the different MRI sequences performed per MRI session. Tapping frequencies were assessed in a subset of 23 participants (6 of the anodal, 7 of the cathodal, and 9 of the sham group) in the first three active blocks within each stimulation condition (pre ctDCS, ctDCS, post ctDCS). Finger movements were counted by one of the experimenters based on visual inspection. A repeated measures ANOVA analysis was performed to compare finger tapping frequencies within and between groups.

Image analyzes

Image analyzes were performed using statistical parametric mapping (SPM) 8 (Wellcome Department of Cognitive Neurology, London, UK, www.fil.ion.ucl.ac.uk/spm/). The EPI images were realigned to correct for head motion, resulting in the creation of a mean EPI image. The first image was selected as a reference, and all images from all paradigms were realigned according to it. Images were manually aligned to the spatially unbiased atlas template (SUIT) of the human cerebellum [22]. The mean image was then used as a reference image to coregister the realigned functional images to the anatomical T1 image of the individual participant. For the first-level statistical analyzes, a general linear model (GLM) was applied [23] to the realigned and coregistered, but otherwise unsmoothed, EPI images. The time series of each voxel was fitted with a corresponding task regressor that modeled a box car convolved with a canonical hemodynamic response function. A temporal high-pass filter (cut off 128 s) was used to correct for low-frequency drifts in the data, and serial autocorrelations were taken into account by means of an autoregressive model first-order correction (AR(1)). First, BOLD effects were compared between motor and resting conditions. Additionally, the following 1st level t-contrasts were calculated: ctDCS > pre ctDCS and post ctDCS > pre ctDCS, as well as the inverse contrasts (pre ctDCS > ctDCS and pre ctDCS > post ctDCS). Comparisons between groups were calculated within respective conditions (pre ctDCS, ctDCS, post ctDCS) at the 2nd level using a full factorial design.

Cerebellar cortex

For the normalization of cerebellar cortical data, the T1-weighted images were deformed to fit the SUIT template of the human cerebellum using the SUIT toolbox in SPM8 [22]. The program initially isolates the cerebellum and creates a mask. For each participant, the mask was manually corrected with the help of MRIcroN software (http://www.sph.sc.edu/comd/rorden/mricron/). Non-linear deformation was then applied to each contrast image. The normalized images were resampled at $1 \times 1 \times 1\,mm^3$ resolution and then smoothed by a 3-D convolution with an isotropic Gaussian kernel of 4-mm full width at half maximum (FWHM). After normalization, second-level statistical analyzes were performed via one-sample t tests. Cerebellar cortical activation is shown at a threshold level of $p < 0.05$, family wise error (FWE) corrected for multiple comparisons with a minimum cluster size of 10 voxels. The probabilistic atlas of the cerebellar cortex was used to define cerebellar lobules [24].

Table 1
Order of MRI sequences.

MRI sequence	duration (min:sec)	Stimulation
fMRI - pre ctDCS	10:00	Off
anatomical MPRAGE	05:08	Off
Resting state - pre ctDCS	10:00	Off
Resting state - ctDCS	10:00	On
fMRI – ctDCS	10:00	On
fMRI – post ctDCS	10:00	Off

Dentate nuclei

The dentate nuclei were identified as hypointensities on the mean image and marked as regions of interest (ROIs) using MRIcroN software. For normalization, a modified version of the SUIT method described above was used. This normalization algorithm deforms the T1 image to fit to the SUIT template, while optimizing the overlap between the ROI and a dentate template [25]. To avoid activation surrounding the dentate nucleus being smoothed into the ROI, the functional images were masked with the dentate ROI before normalization. The normalized functional data from the dentate nuclei were resampled at $1 \times 1 \times 1\,mm^3$ resolution and then smoothed with a 3-D convolution with an isotropic Gaussian kernel of 4 mm. The random field (RF) cluster size correction was not considered suitable for this dataset because the search volume was very small. Bootstrap analysis was therefore used to correct the significance level for multiple tests [26]. Sets of 18 random samples for each group (anodal-, cathodal- and sham-stimulation group) were drawn from all contrast images (with replacement) and multiplied with 1 or −1 to randomize the sign. For each of these simulated datasets, a t-map was calculated and thresholded at $p = 0.01$ uncorrected [$t(17) = 2.60$], searching in both, the left and right dentate nuclei. Following 1000 bootstrapping iterations, the minimum threshold cluster size that would only occur in 5% of the random datasets was determined. The corrected cluster size was 84 voxels for the anodal- and sham-stimulation group and 86 for the cathodal stimulation group.

Transcranial direct current stimulation

For ctDCS, the "DC-Stimulator MR" (NeuroConn, Germany, www.neuroconn.de) was used. This stimulator is compatible with a maximal MRI field strength of 3T and ctDCS can be performed during fMRI acquisition. The tDCS-fMRI setup was arranged as reported previously by Antal et al. [27]. In detail, direct current was provided via a pair of square rubber electrodes ($7 \times 5\,cm^2$). The electrode wires were equipped with 5.6 kΩ resistors to avoid sudden temperature increases due to induction voltages from radio frequency pulses. They were connected to a battery-driven stimulator located outside of the magnet room via a cable running through a radio frequency filter tube in the cabin wall. Two filter boxes were placed between the stimulator and the electrodes. The characteristic bandwidth of the filters on the DC current path was chosen to suppress the MRI radio frequency impulse energy. For cerebellar stimulation, one electrode was centered 3 cm laterally to the inion and the other electrode was placed on the right buccinator muscle [16] prior to MRI scanning. Optimal coverage of the right cerebellar hemisphere was checked in the MRI scout at the beginning of the MRI session. If necessary, electrode position was corrected (Fig. 1). In order to achieve minimum impedance, sponge electrodes were embedded in a saline-soaked solution and conductive electrode paste was placed on the skin (Ten20^R Conductive, Neurodiagnostic Electrode Paste, WEAVER and company, www.weaverandcompany.com/index.html). The intensity of stimulation was set to 1.8 mA. This intensity was chosen because it was the closest intensity to 2 mA which could be applied without exceeding the maximum impedance tolerance (20 kΩ) of the stimulator when using the MRI compatible setup. 2 mA is an

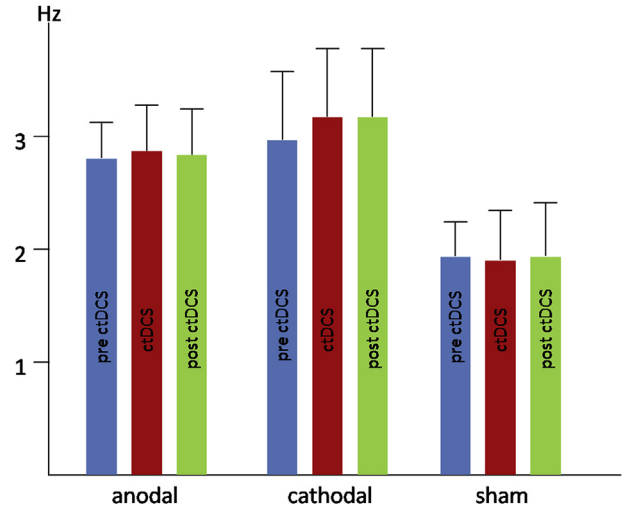

Fig. 2. Tapping frequencies calculated for a subgroup of participants for the anodal, cathodal and sham ctDCS groups. Error bar represents 1 standard deviation.

Table 2
Tapping frequencies in Hz (mean ± standard deviation).

condition/group	pre ctDCS	ctDCS	post ctDCS
Anodal	2.79 ± 0.31	2.88 ± 0.39	2.84 ± 0.40
Cathodal	2.95 ± 0.59	3.15 ± 0.59	3.18 ± 0.61
Sham	1.92 ± 0.31	1.91 ± 0.44	1.93 ± 0.46

intensity which was often used in recent ctDCS studies, and has been shown to induce physiological and functional effects [9,16,28]. For anodal and cathodal stimulation, ctDCS intensity was increased in a ramp-like manner for 30s, kept at 1.8 mA for 20 min and then decreased over 30s again. For the sham stimulation tDCS was increased over 30s as in the anodal and cathodal condition, kept for 40s and then decreased again over 30s. For the remaining time of sham ctDCS, a short ctDCS pulse (110 μA for 15 ms) was applied at 550 ms intervals for impedance control to check electrode contact. This procedure has proven to achieve good blinding to tDCS conditions for participants and investigators [29]. In addition, ctDCS was applied using the „study mode“ of the stimulator, meaning that stimulation conditions were coded in a way that investigators could distinguish between anodal and cathodal stimulation, but not between sham and verum stimulation. After the fMRI experiment, participants were asked to judge whether real or sham ctDCS had been applied. Fisher-Yates-Test was used to compare for possible differences between perceived verum or sham stimulation (yes or no) between study groups.

The tDCS-setup did not influence EPI-image quality regardless of whether the stimulation was turned on or off. This goes in accordance with a previous study by Antal et al. [27] who did not detect alterations of signal to noise ratio (SNR) related to tDCS. Typical examples of EPI images with ctDCS turned on and off are shown in Fig. 1.

Results

Study population

Data of 48 participants (female/male: 23/25, age: 23.8 ± 4.1yrs., mean ± standard deviation) were included in group statistical analyzes. Participants were randomized to anodal stimulation (female/male: 8/8, age: 24.1 ± 3.2yrs.), cathodal stimulation (female/male: 8/8, age: 24.1 ± 4.6yrs.) or sham stimulation (female/male: 7/9, age: 23.4 ± 3.8yrs.) with stratification for age and sex.

Behavioral data

Tapping frequencies are shown in Fig. 2 and Table 2. Repeated measures ANOVA with the factors “stimulation” (pre-, post- and during stimulation) and “group” (anodal, cathodal, sham) revealed no significant difference when comparing the conditions of stimulation ($p > 0.05$). The factor “group” revealed a significant difference ($p = 0.01$). The “stimulation” by “group” interaction was not significant ($p > 0.05$). Tapping frequencies were less in the sham group, as compared to the anodal group ($p < 0.01$; post hoc analysis) and the cathodal group ($p < 0.01$), but did not differ between the anodal and cathodal groups ($p > 0.05$). It cannot be ruled out that verum stimulation increased tapping frequency. However, tapping frequency was not paced and was assessed by visual

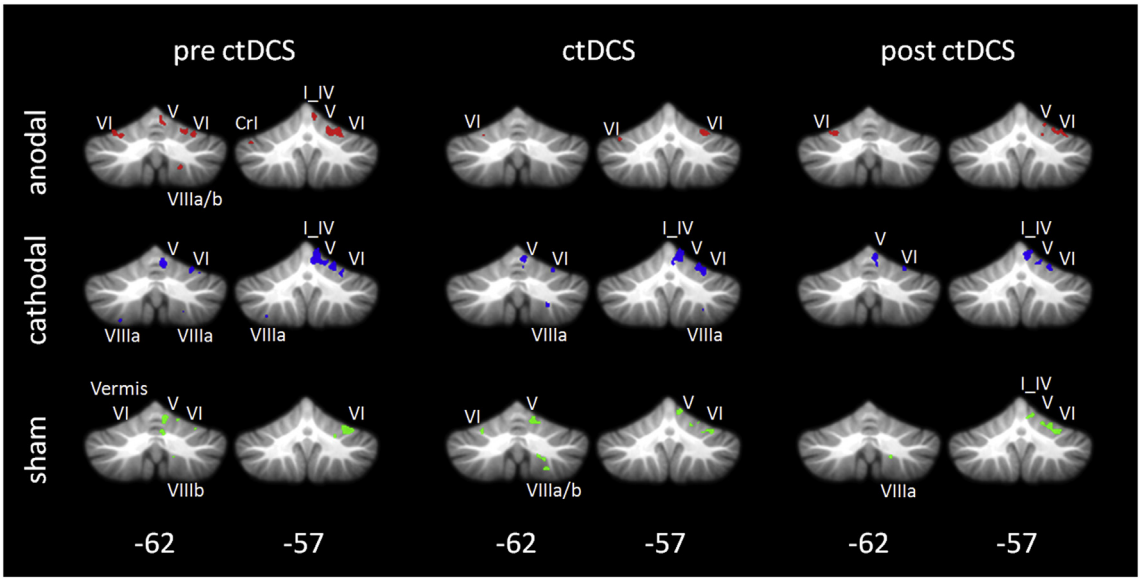

Fig. 3. Cerebellar cortical activations mapped onto the SUIT-template [22] in coronal sections with $p < 0.05$ FWE corrected threshold and minimum cluster size of 10 voxels. White numbers indicate y-coordinates in SUIT space. Roman numbers indicate cerebellar lobules (Cr = Crus). Right side of the image is right side of the brain.

inspection. Therefore a coincidental effect appears most likely. Participants' judgment whether real ctDCS or sham stimulation had been applied (yes or no) was correct in 58,3%, suggesting sufficient blinding. Accordingly, Fisher Yates Test (significance level $p < 0.05$) did not detect a significant difference between study groups.

Cerebellar cortical activation

In general, cerebellar cortical activations (Fig. 3, Table 3) were detected bilaterally, though with a clear accentuation of the right side (ipsilateral to the movement). Activation was present in the known upper-limb motor representation within the anterior (lobules IV, V, VI) and posterior (lobule VIII) cerebellum [30–32]. The pre-stimulation condition showed comparable activation patterns between groups. There was a tendency for lower activation during stimulation and post-stimulation in all groups when compared to the pre-stimulation condition. This may be related to increasing movement automaticity and consecutively decreasing neuronal demands [33]. There were no significant differences between stimulation conditions (that is, pre-, post- and during stimulation) within each group (at a threshold of $p < 0.05$, FWE corrected). In addition, no significant differences were identified between groups (that is, sham, anodal and cathodal stimulation groups) in any of the stimulation conditions ($p < 0.05$, FEW corrected). These results imply that there was no significant effect of ctDCS on cerebellar cortical fMRI activation during performance of the simple motor task.

Table 3
Local activation maxima within the cerebellar cortex ($p < 0.05$, FWE corrected). Peak location is underlined when several lobules are involved. Minimal cluster volume was set to 10 mm^3.

Condition	x,y,z	Location	cluster size (mm^3)	t-value
pre ctDCS (anodal)	20,-49,-16	right: V, VI	1024	14.25
	35,-45,-29	right: VI	89	13.24
	−32,-62,-19	left: VI	122	11.17
	9,-51,-7	right: I_IV	70	10.93
	−42,-58,-29	left: Crus I	28	10.08
	36,-54,-25	right: VI	41	9.54
	19,-62,-48	right: VIIIa, VIIIb	24	9.21
	6,-57,-8	right: V, I_IV	167	9.17
	5,-72,-17	right: vermis VI	11	8.49
pre ctDCS (cathodal)	22,-56,-16	right: VI, I_IV, V, vermis VI	1792	13.24
	29,-61,-18	right: VI	169	13.1
	36,-60,-22	right: VI	48	10.45
	−27,-62,-59	left: VIIIa	15	9.37
	22,-70,-21	right: VI	34	9.34
	33,-53,-28	right: VI	65	9.19
pre ctDCS (sham)	32,-56,-24	right: VI	462	14.87
	−31,-59,-25	left: VI	22	10.18
	7,-61,-26	right: V, vermis VI	40	10.05
	7,-63,-15	right: V	91	10.01
	17,-60,-16	right: V, VI	44	9.99
	23,-56,-28	right: VI	22	9.13
	9,-54,-18	right: V, I_IV	11	8.85
	21,-70,-18	right:VI	12	8.65
ctDCS (anodal)	27,-58,-21	right: VI	153	11.34
	20,-51,-28	right: V, VI	51	10.1
	36,-47,-27	right: VI	79	9.57
	−37,-57,-26	left: VI, CrusI	19	9.47
	24,-59,-49	right: VIIIa	13	9.15
ctDCS (cathodal)	7,-67,-24	right: vermis VI, I_IV, V VI	575	13.57
	27,-59,-20	right: V, VI	793	11.5
	24,-62,-47	right: VIIIa	32	10.34
	39,-54,-25	right: VI	39	9.03
ctDCS (sham)	13,-64,-14	right: V, VI	181	12.24
	34,-56,-25	right: VI	200	11.13
	18,-64,-57	right: VIIIa	67	10.68
	17,-63,-43	right: VIIIa, VIIIb	49	10.55
	17,-51,-26	right: V	73	10.36
	−27,-62,-25	left: VI	26	9.83
	−30,-59,-54	left: VIIIa	17	9.66
	8,-56,-9	right: V	52	9.54
	5,-66,-21	right: vermis VI	22	9.17
	23,-56,-18	right: VI	15	8.63
	27,-60,-19	right: VI	10	8.32
post ctDCS (anodal)	−24,-63,-21	left: VI	62	9.82
	23,-59,-13	right: VI	27	9.71
	26,-56,-18	right: VI	122	9.28
	18,-58,-23	right: V, VI	11	8.1
post ctDCS (cathodal)	16,-54,-14	right: V, VI	759	13.31
	5,-61,-10	right: vermis VI, I_IV, V	464	12.75
post ctDCS (sham)	20,-50,-26	right: V, VI	205	12.54
	7,-55,-14	right: I_IV, V	140	12.07
	30,-54,-28	right: V, VI	309	10.42
	17,-63,-44	right: VIIIa, VIIIb	23	9.95
	6,-66,-16	right: V, VI	20	8.73
	5,-64,-20	right: vermis VI, V	12	8.39

Dentate nucleus activation

For the pre-stimulation condition, no significant cluster was detected in any group, when groups were analyzed separately. Dentate activations were found only at a trend level (7–73 mm^3; Fig. 4, Table 4). During cathodal stimulation and post cathodal stimulation significant clusters were detected. These were located bilaterally during stimulation, and in the right dentate post stimulation. These significant clusters were located in more dorsal parts of the nucleus, the presumed motor-domain [31,34]. No significant clusters were detected in the anodal and sham group both during and post stimulation. On a trend level, dentate activation was observed in the sham conditions and during anodal stimulation (12–56 mm^3). After anodal stimulation, however, dentate activation was even absent on a trend level. Statistical comparisons between stimulation conditions within each group, and comparisons between groups did not reveal significant activations.

Discussion

The most important finding of the present study was that cathodal tDCS of the cerebellum led to a significant increase of the fMRI signal in the dentate nucleus. This finding goes in accordance with the hypothesis that cathodal ctDCS leads to an inhibition of the cerebellar cortex which is followed by disinhibition of the dentate nucleus. Anodal tDCS led to the opposite effect, but only on a trend level.

Cerebellar cortex

Based on the previously reported effects of tDCS on CBI, anodal stimulation was expected to increase the fMRI signal of the cerebellar cortex, whereas cathodal stimulation was expected to decrease the fMRI signal [16]. Contrary to our hypothesis, we did not observe changes of cortical activation, neither following anodal nor cathodal ctDCS. Based on the assumption that ctDCS primarily affects the excitability of Purkinje cells, this result is not fully unexpected. Synaptic activity has been shown to drive the fMRI signal in the cerebellar cortex, but not spiking activity of principle neurons (that is Purkinje cells) [35]. Thus, the mossy and climbing fiber synapses and synaptic connections of the granule cells may contribute the most to the fMRI signal in the cerebellar cortex [36]. At present, however, it is only incompletely understood which cerebellar cell populations are influenced by ctDCS [1]. Evidence from animal studies suggests that Purkinje cells respond to ctDCS [1]. Current flow from the cortical surface to the fourth ventricle leads to excitation of cell bodies and proximal dendrites of Purkinje cells in turtles [37]. However, as yet, it is unknown whether granule cells, the most abundant neuronal population in the cerebellum, and interneurons can be modulated by ctDCS. Future studies are

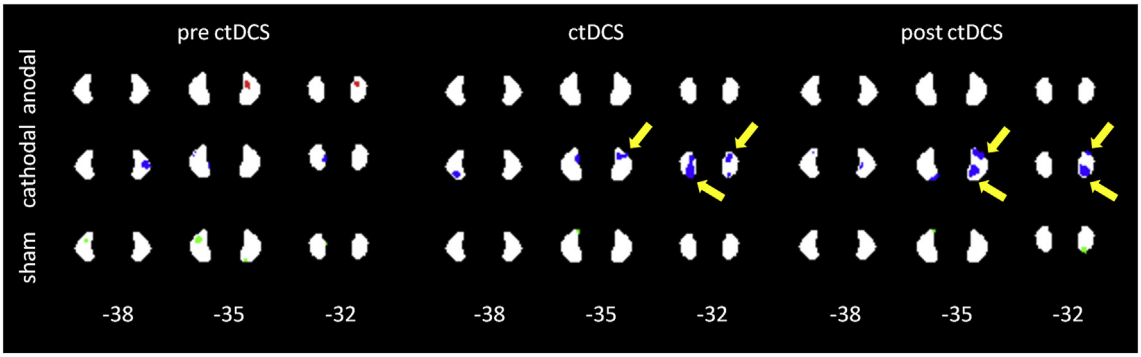

Fig. 4. Dentate nucleus activation mapped onto a probabilistic dentate nucleus template [25] in axial slices (white numbers indicate z-coordinate) thresholded at p = 0.01 (uncorrected). Yellow arrows show significant clusters exceeding a minimum size of 84 (anodal and sham group) or 86 voxels (cathodal group). Right side of the image is right side of the brain. . (For interpretation of the references to colour in this figure legend, the reader is referred to the Web version of this article.)

Table 4
Local maxima of dentate nucleus activations for clusters with a minimum size of 5 voxels thresholded at p = 0.01 (uncorrected). Significant clusters are underlined with a minimum size of 84 voxels for anodal- and sham-stimulation group and 86 for cathodal stimulation group. (n.s.c. = no suprathreshold cluster).

Condition	x,y,z	Location	cluster size (mm^3)	t-value
pre ctDCS (anodal)	11,-56,-33	right dentate	56	4.60
pre ctDCS (cathodal)	−7,-59,-32	left dentate	47	4.80
	19,-58,-38	right dentate	73	3.80
pre ctDCS (sham)	−16,-55,-36	left dentate	47	4.30
	12,-66,-34	right dentate	21	3.02
	−6,-58,-31	left dentate	7	2.83
ctDCS (anodal)	11,-56,-29	right dentate	15	3.26
ctDCS (cathodal)	−11,-61,-31	left dentate	169	5.39
	−16,-63,-39	left dentate	48	4.61
	9,-54,-30	right dentate	118	3.92
	12,-64,-30	right dentate	14	3.19
ctDCS (sham)	−11,-50,-34	left dentate	12	3.56
post ctDCS (anodal)	n. s. c.			
post ctDCS (cathodal)	12,-51,-34	right dentate	94	5.26
	11,-62,-33	right dentate	200	5.05
	−11,-67,-36	left dentate	33	3.27
post ctDCS (sham)	−10,-49,-35	left dentate	11	3.49
	11,-65,-31	right dentate	23	3.13

needed to further elucidate ctDCS effects on the cellular level in the cerebellar cortex.

Furthermore, because ctDCS effects are direction-dependent (alignment of electrical field orientation with neuronal orientation), the highly convoluted cerebellar cortex may lead to opposing effects and hamper the detection of stimulation-related fMRI activity changes. This would also explain why tDCS effects in fMRI studies have been found to be variable [38]. In addition, tDCS effects on fMRI signals may be dependent on the task. For example, Macher et al. (2014) found that anodal ctDCS leads to an attenuated fMRI signal in lobule VII in a verbal working memory task. Therefore, ctDCS effects on fMRI signals may be more prominent in more complex cognitive tasks compared to simple motor tasks, as applied in the current study. Finally, tDCS effects on fMRI signals likely depend on stimulus intensity, and findings may be different using a higher or lower intensity than 1.8 mA (applied in the present study) [39].

Cerebellar nuclei

Electrophysiological studies demonstrated a suppression of CBI by cathodal ctDCS [16]. Our study supports and extends these findings by demonstrating corresponding effects at the level of the dentate nuclei. The fact that dentate nucleus activation was only observed during and after cathodal stimulation is in agreement with the hypothesis that inhibition of the cerebellar nuclei is diminished following cathodal stimulation of the cerebellar cortex. Disinhibition at the dentate level is thought to lead to increased excitation of M1, mediated via the disynaptic excitatory connection between the cerebellar nuclei and M1 via the thalamus. In contrast, dentate activation was absent following anodal ctDCS. This lack of activation is in agreement with the hypothesis that anodal ctDCS results in an increased inhibition of the dentate nuclei.

ctDCS-induced alterations of the fMRI signal may be explained by changes in GABA-levels. Less inhibition of the dentate nucleus goes along with decreased GABA-levels. Decreased GABA-levels correlate with higher fMRI signal responses [40–42]. In accordance, GABA agonists have been shown to reduce local increases in cerebral blood flow [43]. As yet, however, the underlying physiology of the fMRI signal of the cerebellar nuclei has not been studied in detail. Other factors, e.g. increased synaptic activity, are likely to play a role.

It has to be noted that dentate activation in the pre stimulation conditions was weak and observed only at a trend level in the three stimulation groups. Our group has previously reported robust dentate nucleus activation in simple motor tasks [44,45]. These studies, however, have been performed using a 7T MRI system with an increased signal to noise ratio [46] compared to conventional 3T MRI.

In conclusion, the current study provides initial evidence that ctDCS modulates the fMRI signal at the level of the dentate nuclei. Effects of cathodal ctDCS were most prominent, and resulted in increased activation of the dentate nuclei. This observation is in accordance with an inhibitory effect of cathodal ctDCS on the cerebellar cortex resulting in less inhibition of the cerebellar nuclei. The present findings help to explain mechanisms of reduced CBI effects following cathodal ctDCS. Opposite effects of anodal ctDCS were observed, but only on a trend level, and need to be confirmed in future studies. Furthermore, it will be of interest to study changes in functional cerebello-cerebral connectivity in the future to further elucidate the mechanisms of cerebellar tDCS.

Conflicts of interest

None.

Acknowledgments

This work was funded by a research grant awarded to young scientists (M. Thürling) by the DFG Research Unit FOR 1581 and DFG Collaborative Research Center SFB 1280 (Extinction learning; project number 316803389; subprojects A05 and A06).

References

[1] Grimaldi G, Argyropoulos GP, Bastian A, Cortes M, Davis NJ, Edwards DJ, et al. Cerebellar transcranial direct current stimulation (ctDCS): a novel approach to understanding cerebellar function in health and disease. Neurosci Rev J Bringing Neurobiol Neurol Psychiatry 2014. https://doi.org/10.1177/1073858414559409.

[2] Galea JM, Vazquez A, Pasricha N, de Xivry J-JO, Celnik P. Dissociating the roles of the cerebellum and motor cortex during adaptive learning: the motor cortex retains what the cerebellum learns. Cereb Cortex N Y N 1991;21(2011):1761–70. https://doi.org/10.1093/cercor/bhq246.

[3] Hardwick RM, Celnik PA. Cerebellar direct current stimulation enhances motor learning in older adults. Neurobiol Aging 2014;35:2217–21. https://doi.org/10.1016/j.neurobiolaging.2014.03.030.

[4] Herzfeld DJ, Pastor D, Haith AM, Rossetti Y, Shadmehr R, O'Shea J. Contributions of the cerebellum and the motor cortex to acquisition and retention of motor memories. Neuroimage 2014;98:147–58. https://doi.org/10.1016/j.neuroimage.2014.04.076.

[5] Jayaram G, Tang B, Pallegadda R, Vasudevan EVL, Celnik P, Bastian A. Modulating locomotor adaptation with cerebellar stimulation. J Neurophysiol 2012;107:2950–7. https://doi.org/10.1152/jn.00645.2011.

[6] Boehringer A, Macher K, Dukart J, Villringer A, Pleger B. Cerebellar transcranial direct current stimulation modulates verbal working memory. Brain Stimulat 2013;6:649–53. https://doi.org/10.1016/j.brs.2012.10.001.

[7] Ferrucci R, Marceglia S, Vergari M, Cogiamanian F, Mrakic-Sposta S, Mameli F, et al. Cerebellar transcranial direct current stimulation impairs the practice-dependent proficiency increase in working memory. J Cogn Neurosci 2008;20:1687–97. https://doi.org/10.1162/jocn.2008.20112.

[8] Ferrucci R, Brunoni AR, Parazzini M, Vergari M, Rossi E, Fumagalli M, et al. Modulating human procedural learning by cerebellar transcranial direct current stimulation. Cerebellum Lond Engl 2013;12:485–92. https://doi.org/10.1007/s12311-012-0436-9.

[9] Zuchowski ML, Timmann D, Gerwig M. Acquisition of conditioned eyeblink responses is modulated by cerebellar tDCS. Brain Stimulat 2014;7:525–31. https://doi.org/10.1016/j.brs.2014.03.010.

[10] Oldrati V, Schutter DJLG. Targeting the human cerebellum with transcranial direct current stimulation to modulate behavior: a meta-analysis. Cerebellum Lond Engl 2018;17:228–36. https://doi.org/10.1007/s12311-017-0877-2.

[11] Benussi A, Koch G, Cotelli M, Padovani A, Borroni B. Cerebellar transcranial direct current stimulation in patients with ataxia: a double-blind, randomized, sham-controlled study. Mov Disord Off J Mov Disord Soc 2015;30:1701–5. https://doi.org/10.1002/mds.26356.

[12] Grimaldi G, Oulad Ben Taib N, Manto M, Bodranghien F. Marked reduction of cerebellar deficits in upper limbs following transcranial cerebello-cerebral DC stimulation: tremor reduction and re-programming of the timing of antagonist commands. Front Syst Neurosci 2014;8:9. https://doi.org/10.3389/fnsys.2014.00009.

[13] Pozzi NG, Minafra B, Zangaglia R, De Marzi R, Sandrini G, Priori A, et al. Transcranial direct current stimulation (tDCS) of the cortical motor areas in three cases of cerebellar ataxia. Cerebellum Lond Engl 2014;13:109–12. https://doi.org/10.1007/s12311-013-0524-5.

[14] Nitsche MA, Paulus W. Excitability changes induced in the human motor cortex by weak transcranial direct current stimulation. J Physiol 2000;527(Pt 3):633–9.

[15] Nitsche MA, Paulus W. Sustained excitability elevations induced by transcranial DC motor cortex stimulation in humans. Neurology 2001;57:1899–901.

[16] Galea JM, Jayaram G, Ajagbe L, Celnik P. Modulation of cerebellar excitability by polarity-specific noninvasive direct current stimulation. J Neurosci Off J Soc Neurosci 2009;29:9115–22. https://doi.org/10.1523/JNEUROSCI.2184-09.2009.

[17] Kelly RM, Strick PL. Cerebellar loops with motor cortex and prefrontal cortex of a nonhuman primate. J Neurosci Off J Soc Neurosci 2003;23:8432–44.

[18] Ugawa Y, Day BL, Rothwell JC, Thompson PD, Merton PA, Marsden CD. Modulation of motor cortical excitability by electrical stimulation over the cerebellum in man. J Physiol 1991;441:57–72.

[19] Stagg CJ, O'Shea J, Kincses ZT, Woolrich M, Matthews PM, Johansen-Berg H. Modulation of movement-associated cortical activation by transcranial direct current stimulation. Eur J Neurosci 2009;30:1412–23. https://doi.org/10.1111/j.1460-9568.2009.06937.x.

[20] Macher K, Böhringer A, Villringer A, Pleger B. Cerebellar-parietal connections underpin phonological storage. J Neurosci 2014;34:5029–37. https://doi.org/10.1523/JNEUROSCI.0106-14.2014.

[21] Oldfield RC. The assessment and analysis of handedness: the Edinburgh inventory. Neuropsychologia 1971;9:97–113.

[22] Diedrichsen J. A spatially unbiased atlas template of the human cerebellum. Neuroimage 2006;33:127–38. https://doi.org/10.1016/j.neuroimage.2006.05.056.
[23] Friston KJ, Frith CD, Turner R, Frackowiak RS. Characterizing evoked hemodynamics with fMRI. Neuroimage 1995;2:157–65.
[24] Diedrichsen J, Balsters JH, Flavell J, Cussans E, Ramnani N. A probabilistic MR atlas of the human cerebellum. Neuroimage 2009;46:39–46. https://doi.org/10.1016/j.neuroimage.2009.01.045.
[25] Diedrichsen J, Maderwald S, Küper M, Thürling M, Rabe K, Gizewski ER, et al. Imaging the deep cerebellar nuclei: a probabilistic atlas and normalization procedure. Neuroimage 2011;54:1786–94. https://doi.org/10.1016/j.neuroimage.2010.10.035.
[26] Hayasaka S, Nichols TE. Validating cluster size inference: random field and permutation methods. Neuroimage 2003;20:2343–56.
[27] Antal A, Polania R, Schmidt-Samoa C, Dechent P, Paulus W. Transcranial direct current stimulation over the primary motor cortex during fMRI. Neuroimage 2011;55:590–6. https://doi.org/10.1016/j.neuroimage.2010.11.085.
[28] Galea JM, Vazquez A, Pasricha N, de Xivry J-JO, Celnik P. Dissociating the roles of the cerebellum and motor cortex during adaptive learning: the motor cortex retains what the cerebellum learns. Cereb Cortex N Y N 1991;21(2011):1761–70. https://doi.org/10.1093/cercor/bhq246.
[29] Gandiga PC, Hummel FC, Cohen LG. Transcranial DC stimulation (tDCS): a tool for double-blind sham-controlled clinical studies in brain stimulation. Clin Neurophysiol Off J Int Fed Clin Neurophysiol 2006;117:845–50. https://doi.org/10.1016/j.clinph.2005.12.003.
[30] Grodd W, Hülsmann E, Lotze M, Wildgruber D, Erb M. Sensorimotor mapping of the human cerebellum: fMRI evidence of somatotopic organization. Hum Brain Mapp 2001;13:55–73.
[31] Küper M, Thürling M, Stefanescu R, Maderwald S, Roths J, Elles HG, et al. Evidence for a motor somatotopy in the cerebellar dentate nucleus-an fMRI study in humans. Hum Brain Mapp 2011. https://doi.org/10.1002/hbm.21400.
[32] Rijntjes M, Buechel C, Kiebel S, Weiller C. Multiple somatotopic representations in the human cerebellum. Neuroreport 1999;10:3653–8.
[33] Floyer-Lea A, Matthews PM. Changing brain networks for visuomotor control with increased movement automaticity. J Neurophysiol 2004;92:2405–12. https://doi.org/10.1152/jn.01092.2003.
[34] Dum RP, Strick PL. An unfolded map of the cerebellar dentate nucleus and its projections to the cerebral cortex. J Neurophysiol 2003;89:634–9. https://doi.org/10.1152/jn.00626.2002.
[35] Thomsen K, Piilgaard H, Gjedde A, Bonvento G, Lauritzen M. Principal cell spiking, postsynaptic excitation, and oxygen consumption in the rat cerebellar cortex. J Neurophysiol 2009;102:1503–12. https://doi.org/10.1152/jn.00289.2009.
[36] Diedrichsen J, Verstynen T, Schlerf J, Wiestler T. Advances in functional imaging of the human cerebellum. Curr Opin Neurol 2010;23:382–7. https://doi.org/10.1097/WCO.0b013e32833be837.
[37] Chan CY, Nicholson C. Modulation by applied electric fields of Purkinje and stellate cell activity in the isolated turtle cerebellum. J Physiol 1986;371:89–114.
[38] Lindenberg R, Sieg MM, Meinzer M, Nachtigall L, Flöel A. Neural correlates of unihemispheric and bihemispheric motor cortex stimulation in healthy young adults. Neuroimage 2016. https://doi.org/10.1016/j.neuroimage.2016.01.057.
[39] Batsikadze G, Moliadze V, Paulus W, Kuo M-F, Nitsche MA. Partially non-linear stimulation intensity-dependent effects of direct current stimulation on motor cortex excitability in humans. J Physiol 2013;591:1987–2000. https://doi.org/10.1113/jphysiol.2012.249730.
[40] Bednařík P, Tkáč I, Giove F, DiNuzzo M, Deelchand DK, Emir UE, et al. Neurochemical and BOLD responses during neuronal activation measured in the human visual cortex at 7 Tesla. J Cereb Blood Flow Metab Off J Int Soc Cereb Blood Flow Metab 2015;35:601–10. https://doi.org/10.1038/jcbfm.2014.233.
[41] Chen Z, Silva AC, Yang J, Shen J. Elevated endogenous GABA level correlates with decreased fMRI signals in the rat brain during acute inhibition of GABA transaminase. J Neurosci Res 2005;79:383–91. https://doi.org/10.1002/jnr.20364.
[42] Muthukumaraswamy SD, Edden RAE, Jones DK, Swettenham JB, Singh KD. Resting GABA concentration predicts peak gamma frequency and fMRI amplitude in response to visual stimulation in humans. Proc Natl Acad Sci U S A 2009;106:8356–61. https://doi.org/10.1073/pnas.0900728106.
[43] Jessen SB, Brazhe A, Lind BL, Mathiesen C, Thomsen K, Jensen K, et al. GABAA receptor-mediated bidirectional control of synaptic activity, intracellular Ca2+, cerebral blood flow, and oxygen consumption in mouse somatosensory cortex in vivo. Cereb Cortex N Y N 1991;25(2015):2594–609. https://doi.org/10.1093/cercor/bhu058.
[44] Küper M, Dimitrova A, Thürling M, Maderwald S, Roths J, Elles HG, et al. Evidence for a motor and a non-motor domain in the human dentate nucleus–an fMRI study. Neuroimage 2011;54:2612–22. https://doi.org/10.1016/j.neuroimage.2010.11.028.
[45] Küper M, Thürling M, Stefanescu R, Maderwald S, Roths J, Elles HG, et al. Evidence for a motor somatotopy in the cerebellar dentate nucleus-an fMRI study in humans. Hum Brain Mapp 2011. https://doi.org/10.1002/hbm.21400.
[46] Gizewski ER, de Greiff A, Maderwald S, Timmann D, Forsting M, Ladd ME. fMRI at 7 T: whole-brain coverage and signal advantages even infratentorially? Neuroimage 2007;37:761–8. https://doi.org/10.1016/j.neuroimage.2007.06.005.